and warty papules developed mainly on the neck, axillae, groin and perineum. Patients with Hailey–Hailey disease usually develop skin lesions in the third to fourth decade. Histopathology shows primarily suprabasal acantholysis (7).

Although Darier disease and Hailey–Hailey disease are classified as keratinizing and blistering disorders, respectively, two diseases show clinical and histopathological overlaps. In fact, a case of bullous Darier disease mimicking Hailey–Hailey disease was reported (27). The clinicopathological overlap may be due to overlapping roles in the calcium pump proteins. Moreover, these findings suggest that intracellular Ca^{2+} storages play significant roles in regulation of both epidermal cell–cell adhesion and keratinization. Previous studies indicated the importance of extracellular Ca^{2+} in differentiation and cell adhesion in the epidermis. However, a recent study using a combination of two-photon microscopy and phasor analysis of living tissue revealed that free Ca^{2+} in keratinocytes comes from intracellular Ca^{2+} stores in Golgi apparatus and endoplasmic reticulum, rather than form extracellular Ca^{2+} (28).

Inherited skin disorders of epidermal keratins

Keratins are cytoskeletal proteins that provide structural stability and flexibility and thus have a role in maintenance of shape of keratinocytes (29). Keratins are extremely diversified proteins with over 50 functionally different species. Keratins 5 and 14 are the major keratins in basal keratinocytes, while keratins 1 and 10 are expressed in suprabasal layers. Additionally, keratin 2 is expressed in uppermost layers in the epidermis, and keratin 9 is expressed in suprabasal keratinocytes exclusively in the palmoplantar skin. Keratins 6, 16 and 17 are seen specifically in nail, hair, epidermal appendages and palmoplantar epidermis, as well as in healing wounds.

Mutations in these keratins weaken cellular stability and cause destruction of cells by even slight external force, resulting in development of several keratinizing and blistering disorders affecting the skin, mucous membranes, hair and nails (30).

Diseases caused by mutations in the keratin genes include EB simplex, epidermolytic ichthyosis (EI), superficial epidermolytic ichthyosis (SEI), epidermolytic palmoplantar keratoderma (EPPK; Vörner type palmoplantar keratoderma), pachyonychia congenita/focal palmoplantar keratoderma and steatocystoma multiplex (15,31–35). EB simplex was described in the previous section. EI, also known bullous congenital ichthyosiform erythroderma (BCIE) and epidermolytic hyperkeratosis, is an autosomal dominant keratinizing disorder caused by mutations in the *KRT1* or *KRT10* gene (36). Patients with EI frequently show widespread blistering and erosions due to cytoskeletal instability in keratinocytes in the early stage of disease (37). SEI (ichthyosis bullosa of Siemens) is caused by mutations in the *KRT2* gene and is considered to be a milder phenotype of EI (35). EPPK is caused by mutations in the *KRT9* gene (33). Finally, pachyonychia congenita/focal palmoplantar keratoderma is caused by mutations in the *KRT6A-C*, *KRT16* or *KRT17* genes and often shows palmoplantar keratoderma with underlying blister formation (31,32,34). Thus, dysfunction of keratins surely leads to both blisters and abnormal keratinization.

Desmosomes and keratins exert multiple functions in the epidermis

Pemphigus foliaceus is an autoimmune skin blistering disorder characterized by autoantibodies to DSG1, which induce loss of cell–cell adhesion in the epidermis. There are two possible mechanisms for the development of blisters in pemphigus foliaceus. The first hypothesis is anti-DSG1 antibody-dependent steric hindrance of intercellular adhesive site, leading directly to desmosomal dissociation. The other one is antibody-induced intracellular signalling pathways, involving p38 MAPK and c-myc, which also result in loss of cell adhesion (38). Recent *in vitro* study demonstrated an additional role of DSG1 in regulation of epidermal differentiation (39). In this study, decreased expression of DSG1 in the suprabasal epidermis by siRNA was shown to suppress epidermal differentiation and downregulate DSC1, keratin10 and loricrin by suppressing the activity of EGFR-Erk1/2 signalling. This result well explains the finding that palmoplantar hyperkeratosis, but not skin blistering, is induced in striate palmoplantar keratoderma with DSG1 haploinsufficiency.

A heterozygous mutation in keratin 5 or keratin 14 in patients with EB simplex interferes with keratin intermediate filaments, resulting in blisters within basal keratinocytes in response to mild mechanical trauma. Several gene expression studies of EB simplex revealed upregulation in genes encoding epidermal differentiation-related proteins, such as thioredoxin-interacting protein (TXNIP), ANXA8 and DNA-damage-inducible transcript 4 (DDIT4) (40,41). TXNIP interacts with sciellin, a precursor of the cornified envelope, and is assumed to play a role in transition of transient amplifying cells to suprabasal differentiating cells. ANXA8 and DDIT4 have been found to be most abundant in the stratified epithelia, suggesting that they play important roles in keratinocyte differentiation (40). In addition, cultured keratinocytes derived from severe EB simplex showed reduction in components of intercellular junctions, including desmosomes and hemidesmosomes (41). As shown in the previous DSG1 studies (39), downregulation of genes encoding desmosomal proteins may suppress epidermal differentiation. These results may lead to development of palmoplantar keratoderma in adult patients with EB simplex.

Open questions and future perspectives

We overviewed keratinizing and blistering disorders and highlighted the close relationship between the two disease groups. In general, several blistering disorders show abnormal keratinizing skin lesions preferentially on the palms and soles, particularly in the late stage of the disease. In addition, some keratinizing disorders show blistering and erosive skin lesions in early age of the patients, presumably because immature and fragile integrity of the young skin.

The responsible genes for this group of disease encode desmosomal and hemidesmosomal proteins, calcium pumps and keratins. Conversely, there are many keratinizing diseases, which never show blisters and erosions. The responsible genes for this group of disease encode gap junction proteins (connexins), cornified cell envelop–related proteins and enzymes and their inhibitors in the epidermis.

One of the most important and the most difficult questions to be answered is why some keratinizing diseases develop blisters, but others do not? In addition, how such keratinizing diseases develop blister formation in addition to abnormal keratinizing skin lesions?

We have not yet had substantial evidences to answer these crucial questions. However, one clue may be the fact that some of

the diseases showing blisters have mutations in the genes encoding proteins directly related to desmosomal or hemidesmosomal adhesion. Thus, decrease in cell adhesion may lead not only to blister formation but also to abnormal keratinization. It is tempting to speculate that stability of the skin due to strong desmosomal and hemidesmosomal adhesion is required to maintain proper keratinization, and the disruption of the cell adhesion leads to increased turnover of keratinization, resulting in retention of cornified layer.

Similar scenario may be the case in diseases with keratin gene mutations. These diseases also show epidermal instability due to abnormal intracellular keratin networks, which leads to hyperkeratosis. In contrast, in the diseases of calcium pumps, abnormal intracytoplasmic calcium levels may cause both disrupted cell adhesion and abnormal keratinization.

To confirm above speculations, we need more information to be provided by future studies. For example, keratinization and blister formation may be examined by 3D reconstruction study. In the study, human skin is reconstructed from keratinocytes, which are genetically disrupted for one of the possible causative genes described in this review. The results may answer the following questions: (i) Which gene is really responsible for both blistering and keratinizing skin lesions? (ii) Which of abnormal keratinization and blister formation starts earlier? and (iii) How can we correct the abnormality in these disorders simultaneously?

Conclusions

Keratinizing disorders and inherited blistering disorders are known to share some clinical and histopathological features. Recent dermatological researches for these disorders have defined pathogenic mutations in the genes encoding a number of epidermal molecules. These molecules establish a cooperative network in the epidermis and play important roles in regulation of keratinization, cell proliferation and cell–cell adhesion. Future investigations in the field of inherited keratinizing and blistering disorders should provide with many insights into further understanding in keratinocyte biology.

Acknowledgements

We gratefully appreciate the technical assistance of Ms. Hanako Tomita and Ms. Sachika Notomi. This study was supported by Grants-in-Aid for Scientific Research and Strategic Research Basis Formation Supporting Project from the Ministry of Education, Culture, Sports, Science and Technology of Japan and by Health and Labour Sciences Research Grants and grants for Research on Measures for Intractable Diseases from the Ministry of Health, Labour and Welfare of Japan. This work was supported by 'Research on Measures for Intractable Diseases' Project: matching fund subsidy (H23-028) from Ministry of Health, Labour and Welfare. The study was also supported by grants from the Kanae Foundation for the promotion of medical science, Japan Lydia O'Leary Memorial Foundation, Takeda Science Foundation, Uehara Memorial Foundation, Nakatomi Foundation, Kaibara Morikazu Medical Science Promotion Foundation, Cosmetology Research Foundation, Japanese Dermatological Association (Shiseido Award), Fukuoka Foundation for Sound Health and Galderma K.K. (Galderma Award). Dr. Hamada and Dr. Tsuruta made a draft of the manuscript. Dr. Dainichi, Dr. Karashima, Dr. Ohata, Dr. Furumura and Dr. Hashimoto made critical revisions of the manuscript for important intellectual content. Dr. Hamada, Dr. Ishii and Dr. Hashimoto obtained funding. Dr. Fukuda, Dr. Teye and Dr. Numata provided technical or material supports. Dr. Hashimoto supervised the study. All authors approved the final version of the manuscript.

Conflict of interests

There is no conflict of interest.

References

1 Schoop V M, Mirancea N, Fusenig N E. J Invest Dermatol 1999: **112**: 343–353.
2 Akiyama M, Shimizu H. Exp Dermatol 2008: **17**: 373–382.
3 Tsuruta D, Green K J, Getsios S *et al.* Trends Cell Biol 2002: **12**: 355–357.
4 Steinert P M. J Cell Biol 2000: **151**: F5–F8.
5 Ishida-Yamamoto A, Igawa S, Kishibe M. J Dermatol 2011: **38**: 645–654.
6 Lippens S, Hoste E, Vandenabeele P *et al.* Apoptosis 2009: **14**: 549–569.
7 Hamada T, Fukuda S, Ishii N *et al.* Relationship between keratinizaing disorders and inherited blistering disorders. In: Ogawa H, ed. Classification and Treatment of Keratinizing Disorders. Tokyo: Kyowa Kikaku LTD, 2011: 58–61.
8 Dubash A D, Green K J. Curr Biol 2011: **21**: R529–R531.
9 Bolling M C, Jonkman M F. Exp Dermatol 2009: **18**: 658–668.
10 McGrath J A, Mellerio J E. Dermatol Clin 2010: **28**: 125–129.
11 Bragg J, Rizzo C, Mengden S. Dermatol Online J 2008: **14**: 26.
12 Mahoney M G, Sadowski S, Brennan D *et al.* J Invest Dermatol 2010: **130**: 968–978.
13 McGrath J A, McMillan J R, Shemanko C S *et al.* Nat Genet 1997: **17**: 240–244.
14 Jones J C, Hopkinson S B, Goldfinger L E. BioEssays 1998: **20**: 488–494.
15 Sawamura D, Nakano H, Matsuzaki Y. J Dermatol 2010: **37**: 214–219.
16 Fine J D, Eady R A, Bauer E A *et al.* J Am Acad Dermatol 2008: **58**: 931–950.
17 Tsuruta D, Hashimoto T, Hamill K J *et al.* J Dermatol Sci 2011: **62**: 1–7.
18 Hashimoto I, Schnyder U W, Anton-Lamprecht I. Dermatologica 1976: **152**: 72–86.
19 Paller A S, Fine J D, Kaplan S *et al.* Arch Dermatol 1986: **122**: 704–710.
20 Mitsui H, Watanabe T, Komine M *et al.* J Am Acad Dermatol 2005: **52**: 371–373.
21 Meves A, Stremmel C, Gottschalk K *et al.* Trends Cell Biol 2009: **19**: 504–513.
22 Lai-Cheong J E, McGrath J A. Dermatol Clin 2010: **28**: 119–124.
23 Ow C K, Tay Y K. Pediatr Dermatol 2006: **23**: 586–588.
24 Pedace L, Barboni L, Pozzetto E *et al.* Eur J Dermatol 2011: **21**: 334–338.
25 Sakuntabhai A, Ruiz-Perez V, Carter S *et al.* Nat Genet 1999: **21**: 271–277.
26 Hu Z, Bonifas JM, Beech J *et al.* Nat Genet 2000: **24**: 61–65.
27 Kakar B, Kabir S, Garg V K *et al.* Dermatol Online J 2007: **13**: 28.
28 Celli A, Sanchez S, Behne M *et al.* Biophys J 2010: **98**: 911–921.
29 Karantza V. Oncogene 2011: **30**: 127–138.
30 Manabe M. JAMA 2004: **47**: 508–513.
31 Cuperus E, Leguit R J, Sigurdsson V. Eur J Dermatol 2010: **20**: 402–403.
32 Akasaka E, Nakano H, Nakano A *et al.* Br J Dermatol 2011: **165**: 1290–1292.
33 Umegaki N, Nakano H, Tamai K *et al.* Br J Dermatol 2011: **165**: 199–201.
34 McGrath J A. J Invest Dermatol 2011: **131**: 995.
35 Akiyama M, Tsuji-Abe Y, Yanagihara M *et al.* Br J Dermatol 2005: **152**: 1353–1356.
36 Osawa R, Akiyama M, Izumi K *et al.* J Am Acad Dermatol 2011: **64**: 991–993.
37 Klein I, Bergman R, Indelman M *et al.* Int J Dermatol 2004: **43**: 295–297.
38 Amagai M, Stanley J R. J Invest Dermatol 2012: **132**: 776–784.
39 Getsios S, Simpson C L, Kojima S *et al.* J Cell Biol 2009: **185**: 1243–1258.
40 Wagner M, Hintner H, Bauer J W *et al.* Exp Dermatol 2012: **21**: 111–117.
41 Liovic M, D'Alessandro M, Tomic-Canic M *et al.* Exp Cell Res 2009: **315**: 2995–3003.

The American Journal of Pathology, Vol. 182, No. 3, March 2013

ELSEVIER

The American Journal of
PATHOLOGY

ajp.amjpathol.org

IMMUNOPATHOLOGY AND INFECTIOUS DISEASES

Bullous Pemphigoid IgG Induces BP180 Internalization via a Macropinocytic Pathway

Sho Hiroyasu,* Toshiyuki Ozawa,† Hiromi Kobayashi,* Masamitsu Ishii,* Yumi Aoyama,‡ Yasuo Kitajima,§ Takashi Hashimoto,¶ Jonathan C.R. Jones,‖ and Daisuke Tsuruta*¶

From the Departments of Dermatology and Plastic and Reconstructive Surgery,† Osaka City University Graduate School of Medicine, Osaka, Japan; the Department of Dermatology,‡ Okayama University Graduate School of Medicine, Okayama, Japan; the Division of Dermatology,§ Kizawa Memorial Hospital, Gifu, Japan; the Department of Dermatology,¶ Kurume University School of Medicine, and Kurume University Institute of Cutaneous Cell Biology, Fukuoka, Japan; and the Department of Cell and Molecular Biology,‖ Northwestern University the Feinberg School of Medicine, Chicago, Illinois*

Accepted for publication November 14, 2012.

Address correspondence to Daisuke Tsuruta, M.D., Ph.D., Department of Dermatology, Osaka City University Graduate School of Medicine, 1-4-3 Asahimachi, Abeno-ku, Osaka 545-8585, Japan. E-mail: dtsuruta@med.osaka-cu.ac.jp.

Bullous pemphigoid (BP) is an autoimmune blistering skin disease induced by pathogenic autoantibodies against a type II transmembrane protein (BP180, collagen type XVII, or BPAG2). In animal models, BP180 autoantibody-antigen interaction appears insufficient to develop blisters, but involvement of complement and neutrophils is required. However, cultured keratinocytes treated with BP-IgG exhibit a reduction in the adhesive strength and a loss of expression of BP180, suggesting that the autoantibodies directly affect epidermal cell—extracellular matrix integrity. In this study, we explored the consequences of two distinct epithelial cells treated with BP-IgG, particularly the fate of BP180. First, we followed the distribution of green fluorescent protein—tagged BP180 in an epithelial cell line, 804G, and normal human epidermal keratinocytes after autoantibody clustering. After BP-IgG treatment, the adhesive strength of the cells to their substrate was decreased, and BP180 was internalized in both cell types, together with the early endosomal antigen-1. By using various endocytosis inhibitors and a fluid-uptake assay, we demonstrated that BP-IgG—induced BP180 internalization is mediated via a macropinocytic pathway. Moreover, a macropinocytosis inhibitor rescued a BP-IgG—induced reduction in the adhesive strength of the cells from their substrate. The results of this study suggest that BP180 internalization induced by BP-IgG plays an important role in the initiation of disease pathogenesis. *(Am J Pathol 2013, 182: 828—840; http://dx.doi.org/10.1016/j.ajpath.2012.11.029)*

Bullous pemphigoid (BP) is one of the most common autoimmune blistering diseases and is characterized by tense inflammatory subepidermal bullae caused by anti-basement membrane zone autoantibodies.[1,2] BP autoantigens are two major hemidesmosomal components, BP180/type XVII collagen/BPAG2 and BP230/BPAG1e.[3–6]

Whether anti-BP230 autoantibodies directly contribute to BP pathogenesis is controversial.[7,8] In contrast, several studies using experimental animal models have suggested that IgG anti-BP180 antibodies contribute to BP blister formation. Specifically, passive transfer of rabbit IgG antibodies against the murine homologue of human BP180 NC16A into healthy mice induces subepidermal blisters.[9] Moreover, injection of IgG anti-human BP180 antibodies induces subepidermal blisters in BP180-knockout mice engineered to express human BP180.[10]

Although there is overwhelming evidence that binding of anti-BP180 autoantibodies to BP180 initiates disease, such antibody-antigen interaction appears insufficient to induce blisters in various BP animal models. Indeed, there is evidence that BP pathogenesis requires activation of complement and the presence of neutrophils and mast cells, although the role of mast cells has been questioned by a recent study.[11–14] BP autoantibodies binding to hemidesmosomes are assumed not to disrupt epidermal cell-connective tissue interaction. However, contrary to this assumption, recent studies indicate that cultured keratinocytes treated with IgG

Supported by The Osaka Medical Research Foundation for Intractable Diseases grant 15-23 (S.H.), the Japanese Dermatological Association Shiseido Award 23-13, the Ministry of Education, Culture, Sports, Science and Technology of Japan Grants-in-Aid for Science Research and Strategic Research Basis Formation Supporting Project J112640081 (D.T.), and NIH grant R01 AR054184 (J.C.R.J.).

http://dx.doi.org/10.1016/j.ajpath.2012.11.029

from patients with BP (BP-IgG) exhibit a reduction in the adhesive strength and a loss in BP180 expression.[15,16] Moreover, we have demonstrated that the velocity of keratinocytes is increased by BP-IgG treatment *in vitro*.[17] These findings raise the question as to how BP autoantibodies influence keratinocyte adhesion and migration without involvement of various inflammatory processes. Hence, in this study, we examined the functions of BP-IgG by following the fate of green fluorescent protein (GFP)—tagged full-length BP180 (GFP-BP180) after BP-IgG treatment in live 804G epithelial cells, which are known to assemble bona fide hemidesmosomes,[18] and normal human epidermal keratinocytes (NHEKs).

Materials and Methods

IgGs from Patients with BP

In accordance with Osaka City University Hospital (Osaka, Japan) and Kurume University Hospital (Fukuoka, Japan) bylaws, we obtained patient consent for experimental procedures to be performed in Osaka City University Hospital and Kurume University Hospital from each participating patient on his or her first visit to the hospital. BP-IgGs were purified from the serum samples of 20 patients with BP who were diagnosed as having BP based on the presence of typical clinical, histological, and immunopathological findings. Their enzyme-linked immunosorbent assay (ELISA) index values for BP180 NC16A autoantibodies were >100, whereas their ELISA index values for BP230 autoantibodies did not exceed 6. ELISAs were performed using commercial kits (MESACUP BP180 test and BP230 ELISA kit; MBL, Nagoya, Japan). IgGs were affinity purified from the serum samples using HiTrap Protein G HP Columns (GE Healthcare, Buckinghamshire, UK). The medical ethical committee of Osaka City University approved all studies performed in this study. The study was conducted according to the principles of the Declaration of Helsinki.

Preparation of HiLyte Fluor 647—Conjugated IgG and IgG F(ab′)2 and IgG Fab Fragments

HiLyte Fluor 647—conjugated BP-IgG and nonpathological IgG were prepared using the HiLyte Fluor 647 Labeling Kit-NH2 (Dojindo, Kumamoto, Japan), according to the manufacturer's protocol. BP-IgG F(ab′)2 and BP-IgG Fab fragments were generated by pepsin and papain, respectively, using commercial kits (Pierce, Rockford, IL), according to the manufacturer's protocols.

Antibodies and Immunofluorescence Probes

The rabbit anti-GFP monoclonal antibody (mAb; A11122) was obtained from Invitrogen (Carlsbad, CA). The horseradish peroxidase—conjugated goat anti-rabbit IgG polyclonal antibody (pAb) was purchased from KPL (Gaithersburg, MD). The rat mAb GoH3, a blocking antibody directed against the extracellular portion of human α6 integrin, was obtained from eBioscience (San Diego, CA). The mouse mAb 3E1 (MAB1964), a blocking antibody against human β4 integrin, was purchased from Millipore (Billerica, MA). The mouse anti-human β4 integrin mAb (555722) was purchased from BD Biosciences (San Diego, CA). The mouse anti-rat β4 integrin (ab29042) was purchased from AbCam (Cambridge, UK). The methods for the production and characterization of 5E, a human mAb against BP230, mAb-233, a mouse mAb against the extracellular domain of BP180, and J17, a rabbit pAb against the N-terminal domain of BP180, were described elsewhere.[19–22] The antibodies 610457 (BD Biosciences), 610500 (BD Biosciences), and 3238 (Cell Signaling Technology Inc., Beverly, MA) recognize early endosomal antigen-1 (EEA-1), clathrin, and caveolin-1, respectively. The Alexa Fluor (AF) 488— and AF 597—labeled secondary antibodies were obtained from Invitrogen. The mouse anti-EGFR pAb (ab2430) was purchased from AbCam.

Cells and Culture Conditions

The 804G cells were cultured in Dulbecco's modified Eagle's medium (Invitrogen), supplemented with 10% fetal bovine serum (Invitrogen) and 50 U/mL penicillin and 50 μg/mL streptomycin at 37°C, in a humidified atmosphere containing 5% CO_2. NHEKs from neonate (Invitrogen) were cultured first in HuMedia-KG2 (Kurabo, Osaka, Japan). When used for experiments, NHEKs were cultured in HuMedia-KG2 containing 1.8 mmol/L $CaCl_2$ for 12 to 24 hours.

IgG Stimulation

To examine the function of BP-IgG in 804G cells and NHEKs, BP-IgG and normal IgG were added at final concentrations of 2.0 mg/mL in the culture media. Final concentrations of GoH3 and 3E1 were 30 μg/mL in the culture media. Final concentrations of 1.47 mg/mL BP-IgG F(ab′)2 and 1.33 mg/mL BP-IgG Fab fragments in the culture media were used in certain studies.

Endocytosis Inhibitors

The 1 mmol/L *N*-ethylmaleimide (NEM; Sigma-Aldrich, St. Louis, MO), 0.4 mol/L sucrose (Sigma-Aldrich), 50 μmol/L nystatin (Sigma-Aldrich), 100 μmol/L genistein (Wako, Osaka, Japan), 2 μmol/L cytochalasin D (Sigma-Aldrich), and 200 μmol/L 5-(*N*-ethyl-*N*-isopropyl) amiloride (EIPA; Sigma-Aldrich) were added in the culture media 30 minutes before the experiments (except for nystatin with 1-hour treatment). The effects of these inhibitors of general, clathrin-dependent, and caveolae-dependent endocytosis were confirmed by preliminary experiments using 804G cells, which were incubated with 1 μg/mL recombinant rat EGF

(R&G Systems, Inc., Minneapolis, MN) for 1 hour to trigger EGFR internalization, a typical clathrin-dependent endocytic event, or with 3 μg/mL AF 594–conjugated cholera toxin subunit B (CTB; Invitrogen) for 30 minutes to trigger internalization of CTB itself, a typical caveolae-dependent endocytosis. EGFR was visualized by immunofluorescence staining with anti-EGFR pAb, and AF 594–conjugated CTB was monitored directly by a TCS SP5 confocal microscope (Leica Microsystems, Mannheim, Germany), after treatment with the indicated inhibitors. Microscope images were exported as .tif files, and figures were generated using Adobe Photoshop CS5 (Adobe Systems, San Jose, CA).

Immunofluorescence Analyses

The cells grown on glass coverslips were fixed in 3.7% formaldehyde in PBS for 8 minutes, washed thoroughly in PBS, and permeabilized in 0.1% (v/v) Triton X-100 in PBS for 10 minutes. Primary antibodies were overlaid onto the cells, and the preparations were incubated at 37°C for 1 hour. The cells on coverslips were washed with PBS, and conjugated secondary antibodies were applied for 1 hour at 37°C. After being washed with PBS, coverslips were mounted onto slides. All preparations were examined by the TCS SP5 confocal microscope.

Western Blot and SDS-PAGE Analyses

For Western blot analyses of whole-cell lysates, the cells were lysed in RIPA Lysis buffer (Upstate, Lake Placid, NY) and boiled in NuPAGE LDS sample buffer (Invitrogen) containing 2.5% 2-mercaptoethanol (Wako). Each sample was processed for SDS-PAGE in 3% to 8% NuPAGE Tris-Acetate Mini Gels (Invitrogen). The separated proteins were transferred to Hybond-P polyvinylidene difluoride membranes (GE Healthcare). These membranes were probed with anti-GFP antibody or J17, washed, and probed with horseradish peroxidase–conjugated goat anti-rabbit pAb. Signals were detected with Super Signal West Dura Substrate (Thermo Fisher Scientific, Rockford, IL).

Samples of F(ab′)2 and Fab fragments in LDS sample buffer were processed for SDS-PAGE in 4% to 12% NuPAGE Bis-Tris Mini Gels (Invitrogen) to confirm the absence of the undigested IgG in the solutions. The membrane, to which the proteins were transferred, was stained with amido-black (Sigma-Aldrich).

Plasmid Constructs

mRNAs were extracted from subconfluent cultures of NHEKs using the RNeasy Plus Mini Kit (Qiagen, Mississauga, ON, Canada), and cDNAs were generated using the High Capacity cDNA reverse transcription kit (Applied Biosystems, Foster City, CA). cDNAs encoding the 5′ half and 3′ half of human BP180 were generated by PCR from the cDNA library using the following primers: 5′-CGCGGATCCATGGARGRAACCAAGAAAAACAA-3′ (forward) and 5′-TTCACCTTTTATTCCTGGTCG-3′ (reverse) and 5′-CCCAAGCTTCGGCTTGACAGCAATACT-3′ (forward) and 5′-AGGAAAGCCAGGTCTCACAG-3′ (reverse), respectively. After gel purification and restriction digestion with BamHI, KpnI, and NotI, both cDNA fragments were ligated into the BamHI/NotI sites of Kikume Green-Red, mammalian expression vector (MBL). The construct was sequenced using the ABI3130xl sequencer (Applied Biosystems) to ensure that it was in frame and had no errors. After restriction digestion with NheI, NotI, and DraI, the cDNA fragments were ligated into the NheI/NotI

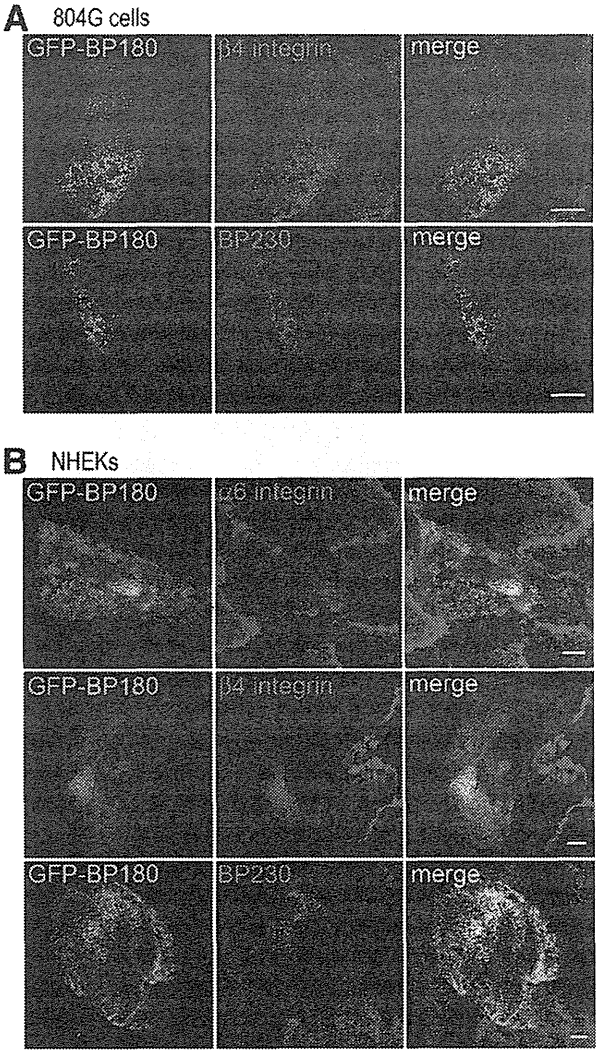

Figure 1 GFP-BP180 incorporates into hemidesmosome-like structures in 804G cells and NHEKs. **A:** GFP-BP180–expressing 804G cells were stained using antibody against rat β4 integrin or 5E antibody against BP230. GFP-BP180 localized precisely with β4 integrin and BP230 in a cat paw–like pattern at the substratum-attached surface. **B:** Immunofluorescence analyses of GFP-BP180–expressing NHEKs using GoH3 mAb against human α6 integrin, antibody against human β4 integrin, or 5E antibody against BP230. GFP-BP180 colocalized with other hemidesmosomal components. Scale bars: 10 μm.

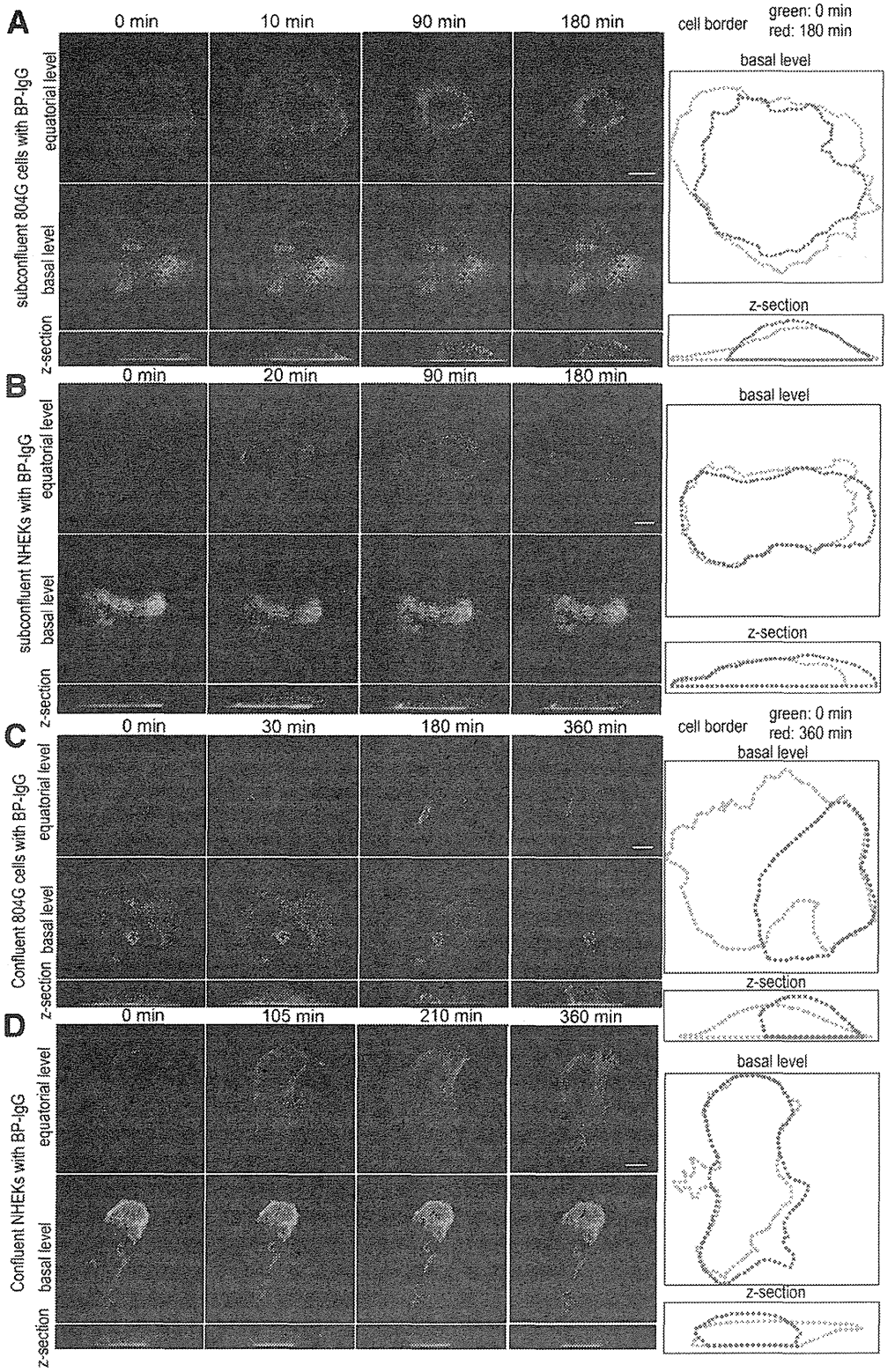

Figure 2 BP-IgG–induced GFP-BP180 internalization in live 804G cells and NHEKs. Live cell imaging studies of subconfluent (**A**) and confluent (**C**) cultures of 804G cells and subconfluent (**B**) and confluent (**D**) cultures of NHEKs. GFP-BP180–expressing cells were visualized by confocal microscopy, either along their substrate-attached surface (basal level) or at a higher focal plane (equatorial level), at various intervals after BP-IgG treatment. In both cell types and conditions, GFP-BP180 was internalized and redistributed centripetally toward the perinuclear region (**A**–**D**). Z-sections of the cells are shown at the bottom of each column. At the right, images of the cell border at time 0 and the end of the observation are shown in green and red, respectively. In 804G cells, rounding up of the cells was observed (**A** and **C**). Scale bars: 10 μm.

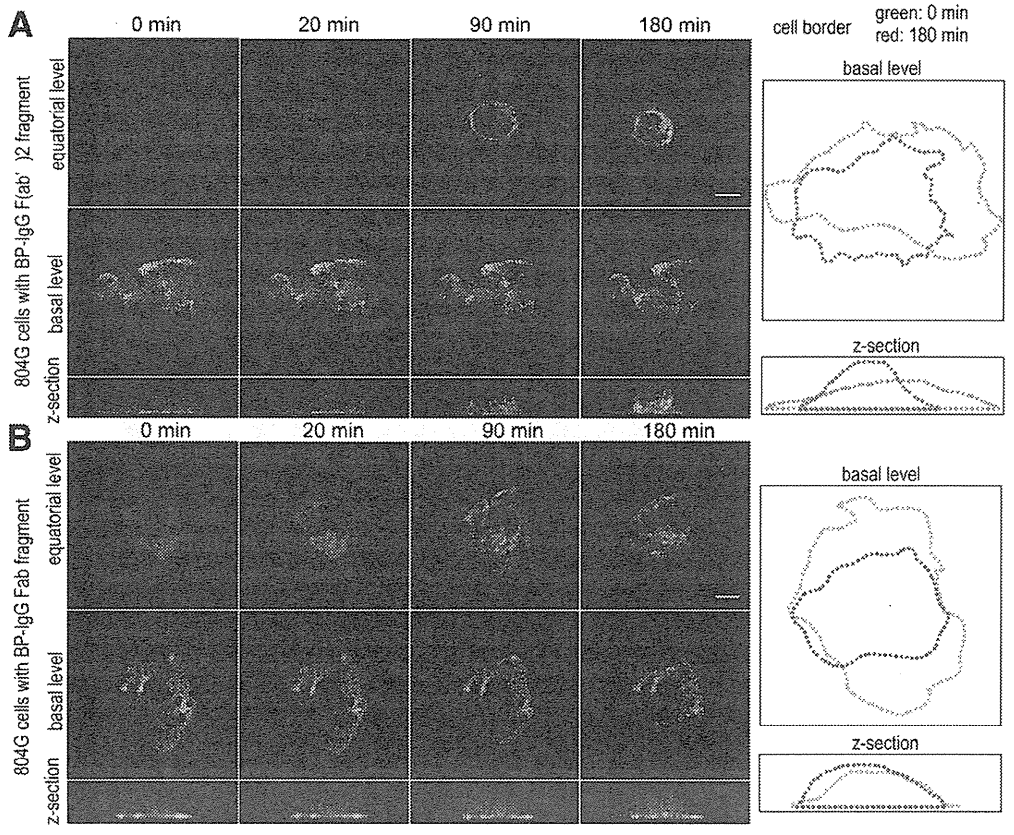

Figure 3 BP-IgG F(ab')2 and BP-IgG Fab fragments induce GFP-BP180 internalization in live 804G cells. Live cell imaging studies of subconfluent cultures of 804G cells treated with BP-IgG F(ab')2 (**A**) and BP-IgG Fab (**B**) fragments. GFP-BP180 was internalized and redistributed centripetally toward the perinuclear region after treatment with both fragments. The fragments induced some cell rounding, as indicated by the outlines of the treated cells at times 0 and 180 minutes, shown to the right. Scale bars: 10 μm.

site of pcDNA 3.1/NT-GFP-TOPO mammalian expression vector (Invitrogen). A stop codon was inserted at the end of the part of BP180 by a KOD mutagenesis kit (Toyobo, Osaka, Japan) using a forward primer, 5′-TGAAAGGGC-GAATTCTGCAGATATCCATCACA-3′, and a reverse primer, 5′-CGGCTTGACAGCAATACTTCTTCTCCTTC-TC-3′, and the final clone was designated GFP-BP180. GFP-BP180 was sequenced again to ensure that it was in frame and had no errors. A construct PmKate2-zyxin was purchased from Evrogen (Moscow, Russia). A construct encoding GFP-tagged β4 integrin was characterized elsewhere.[23]

Transfection Procedures

At 24 hours before transfection, the culture media for 804G cells and NHEKs were changed to Dulbecco's modified Eagle's medium and HuMedia without antibiotics, respectively. Transfections were performed using the Lipofectamine 2000 reagent (Invitrogen) or polyethyleneimine (Sigma-Aldrich) in OPTI-MEM (Gibco, Grand Island, NY) with the vectors. Six hours later, the media were replaced with normal media. At 24 hours after transfection, the cells were suspended and seeded onto triple-well glass-bottomed dishes (Asahi Techno Glass Co, Tokyo, Japan). At 24 hours after seeding, 804G cells were immediately processed for live cell imaging, whereas NHEKs were further cultured in high Ca^{2+} medium for 12 to 24 hours before imaging. For Western blot analyses, GFP-positive NHEKs were sorted by using an FACS Vantage SE sorter (BD Biosciences), whereas transfected 804G cells were selected in 1000 μg/mL G418 (Sigma-Aldrich).

Live Cell Imaging

Time-lapse microscopy of the cells on triple-well glass-bottomed dishes was performed with the confocal laser scanning microscope, type TCS SP5. Subconfluent cultures of the cells were scanned every 5 minutes, and confluent cultures were scanned every 15 or 30 minutes.

Fluid-Phase Uptake Assay

Subconfluent cultures of GFP-BP180–transfected 804G cells on glass-bottomed dishes were incubated with 2.0 mg/mL BP-IgG and 0.5 mg/mL 10-kDa dextran–AF 594 (Invitrogen), a fluid-phase marker, for 10 minutes. The cells were fixed in 3.7% formaldehyde in PBS for 8 minutes. After being washed with PBS, the cells were observed with the TCS SP5 confocal microscope.

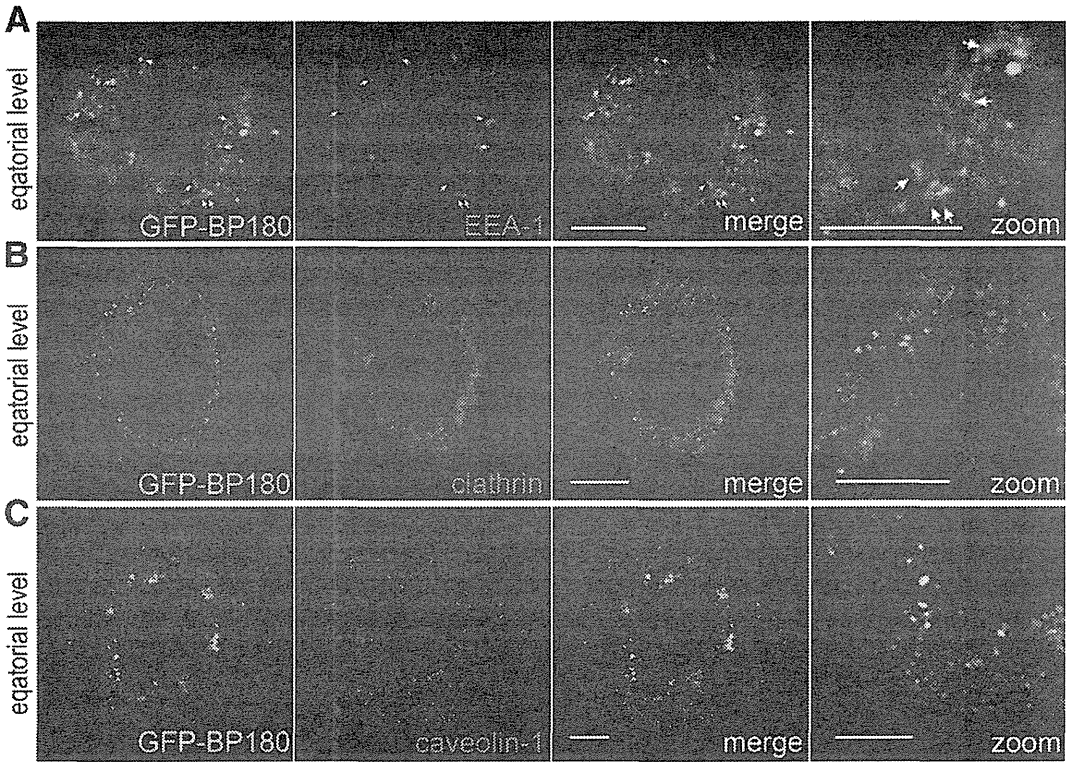

Figure 4 BP-IgG–induced GFP-BP180 internalization is mediated through endocytosis. **A**: After the incubation with BP-IgG for 1 hour, GFP-BP180–expressing 804G cells were stained for EEA-1, which showed some colocalization with GFP-BP180 in the cytoplasm (**arrows**). In contrast, after a 2-hour incubation with BP-IgG, GFP failed to colocalize with either clathrin (**B**) or caveolin-1 (**C**). Scale bars: 5 μm.

Detachment of Colonies from the Bottom of the Culture Plate

The strength of adhesion was measured as previously detailed.[15] Briefly, NHEKs cultured for 50 hours were treated with 2.0 mg/mL BP-IgG or normal IgG for 6 hours, followed by pre-incubation with or without EIPA for 30 minutes. After vortex mixing for 30 minutes, the numbers of attached cells were counted.

Statistical Analysis

Data are expressed as means ± SDs from three different measurements for individual samples from five different experiments. Statistical significance was determined by the Student's *t*-test. $P \leq 0.01$ was considered significant.

Results

GFP-BP180 Expression in 804G Cells and NHEKs without BP-IgG Treatment

In 804G cells, transfected GFP-BP180 codistributed with other hemidesmosomal components, including β4 integrin and BP230, in a cat paw–like pattern at the substratum-attached surface of the cells (Figure 1A). In NHEKs, transfected GFP-BP180 mainly localized at the substratum-attached surface of the cells, where it colocalized with α6 integrin, β4 integrin, and BP230 (Figure 1B). Western blot analyses of extracts from the GFP-BP180–transfected 804G cells and NHEKs were performed to confirm the appropriate expression of GFP-BP180 protein. In transfected 804G cells, anti-BP180 antibody recognized strongly endogenous BP180 and weakly a 207-kDa polypeptide consistent with recombinant BP180 fused with a 27-kDa GFP tag, whereas anti-GFP mAb recognized only the 207-kDa recombinant BP180 (Supplemental Figure S1A). In transfected NHEKs, a similar expression pattern was found (Supplemental Figure S1B).

BP-IgG Treatment Induces an Internalization of GFP-BP180

To observe the dynamics of BP-IgG–bound BP180, we followed GFP-BP180 in subconfluent cultures of 804G cells by live cell imaging, after treatment with BP-IgG at a concentration of 2.0 mg/mL (Figure 2A and Supplemental Movie S1). Before BP-IgG treatment, GFP-BP180 localized mainly at the substratum-attached surface of the cells in a distinct patch-like pattern, whereas some GFP-BP180 localized diffusely in the cytoplasm. Approximately 10 minutes after BP-IgG treatment, GFP-BP180 was detected in the cytoplasm as defined spots. By 90 minutes,

GFP-BP180—positive cytoplasmic inclusions redistributed centripetally toward the perinuclear region. Interestingly, the patches of GFP-BP180 localized along the substratum-attached surface of the cell maintained their form throughout the observation period (up to 180 minutes). At 180 minutes after treatment with BP-IgG, the cells rounded up (Figure 2A). However, the treated cells did not detach from the dish during the observation period. There was neither obvious GFP-BP180 dynamic movement nor observable morphological changes in subconfluent cultures of 804G cells treated with normal IgG during the same time period (Supplemental Figure S2A).

In subconfluent cultures of NHEKs treated with BP-IgG, GFP-BP180 was internalized from the substratum-attached surface into the cytoplasm as spot-like structures within approximately 20 minutes (Figure 2B and Supplemental Movie S2). Most of the internalized GFP-BP180 showed a centripetal redistribution by 90 minutes. Compared with the results in 804G cells, less GFP-BP180 localized in the cytoplasm at 180 minutes after BP-IgG treatment. The cells did not show obvious rounding up at 180 minutes after BP-IgG treatment, in contrast to what was observed under the same conditions using 804G cells (Figure 2B). Control IgG showed no particular effects on GFP-BP180 expression and the morphological characteristics in NHEKs (Supplemental Figure S2B).

GFP-BP180 expressed in NHEKs treated with inhibitory antibodies against the hemidesmosome proteins α6 integrin (GoH3) or β4 integrin (3E1) failed to become cytoplasmic, although the treated cells changed shapes and partially detached from their substrate (Supplemental Figure S2, C and D). Moreover, in NHEKs expressing either GFP-tagged β4 integrin or pmKate2-zyxin, a focal contact component, there was no internalization of either tagged protein after BP-IgG treatment (Supplemental Figure S2, E and F). However, the amount of tagged zyxin was reduced at 135 minutes after BP-IgG treatment.

Next, we followed the fate of GFP-BP180 for 6 hours in confluent cultures of 804G cells and NHEKs treated with BP-IgG (Figure 2, C and D, and Supplemental Movies S3 and S4). GFP-BP180 was internalized, as was the case in subconfluent cultures, although the time course and the numbers of internalized dot-like structures were distinct.

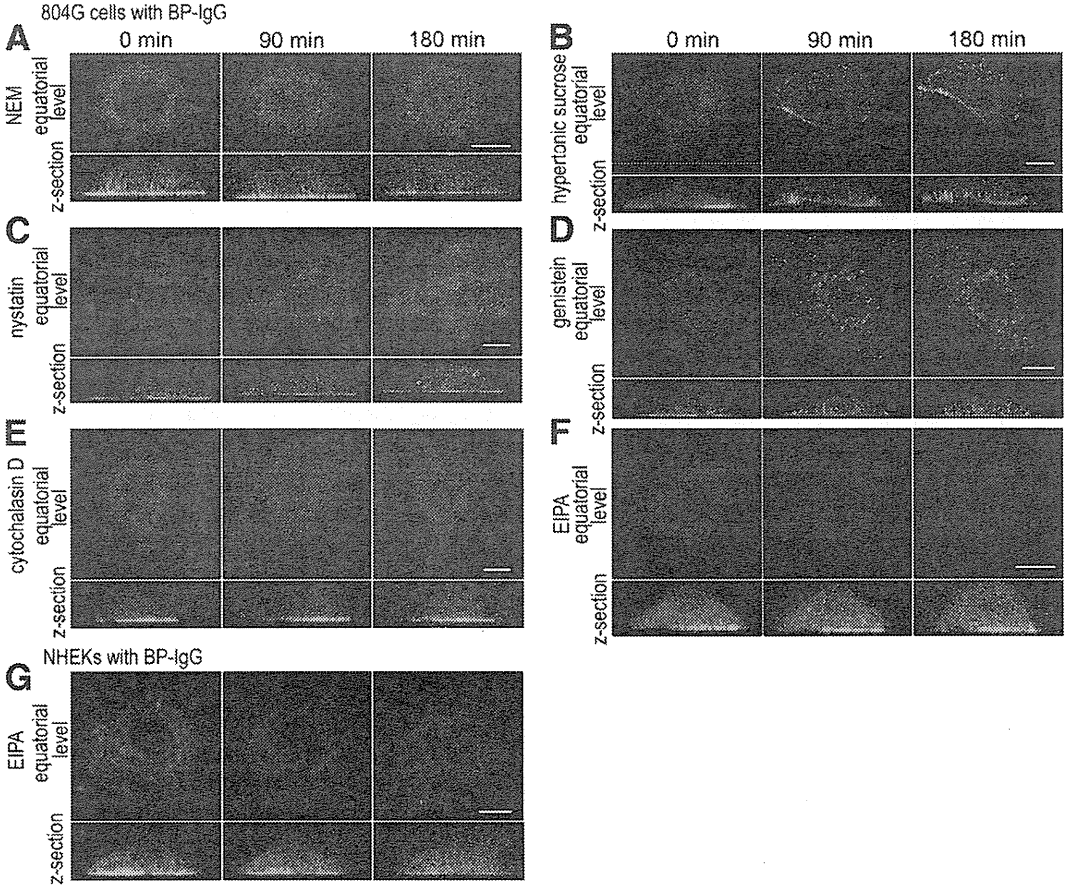

Figure 5 Pre-incubation with the inhibitors of general endocytosis and macropinocytosis prevents BP-IgG–induced GFP-BP180 internalization. Live cell imaging studies for GFP-BP180–expressing 804G cells (**A**–**F**) and NHEKs (**G**) treated with BP-IgG and endocytosis inhibitors. **A:** Pre-incubation with NEM inhibited BP-IgG–induced GFP-BP180 internalization and cell morphological changes in 804G cells. Hypertonic sucrose (**B**), nystatin (**C**), and genistein (**D**) failed to prevent GFP-BP180 internalization in BP-IgG–treated 804G cells. Cytochalasin D (**E**) and EIPA (**F**) inhibited GFP-BP180 internalization in 804G cells. **G:** In NHEKs, EIPA prevented BP-IgG–induced GFP-BP180 internalization at 180 minutes. Scale bars:10 μm.

GFP-BP180 was internalized in confluent cultures of 804G cells and NHEKs within 30 and 105 minutes, respectively, after treatment with BP-IgG. Moreover, in both 804G cells and NHEKs, a centripetal redistribution of GFP-BP180 was observed at 180 and 210 minutes, respectively. Compared with our observations on subconfluent cultures, less GFP-BP180 was internalized in confluent cultures of both cell types after BP-IgG treatment. As was the case in subconfluent cultures, BP-IgG–induced cell rounding of NHEKs in confluent cultures had a much less dramatic effect than that of 804G cells in confluent cultures (Figure 2, C and D).

Treatments with BP-IgG F(ab′)2 and BP-IgG Fab Fragments Induce an Internalization of GFP-BP180

The live cell imaging observations shown in Figure 2 suggested that BP-IgG treatment induces BP180 internalization. If it was mediated through a noninflammatory pathway, the Fc portion of BP-IgG might not be required. Therefore, we next examined whether GFP-BP180 is internalized after treatments with BP-IgG F(ab′)2 and BP-IgG Fab fragments. To generate F(ab′)2 and Fab fragments, BP-IgG was digested by pepsin and papain, respectively. We confirmed the absence of undigested IgG and the high purity of F(ab′)2 and Fab fragments by SDS-PAGE (Supplemental Figure S3). Live cell imaging observations confirmed that both F(ab′)2 and Fab fragments induced GFP-BP180 internalization in subconfluent cultures of 804G cells (Figure 3, A and B). The results suggested that BP-IgG–induced BP180 internalization is regulated by an FcR-independent mechanism. For this and some following studies, we used only GFP-BP180–expressing 804G cells, because these cells showed a more prominent internalized tagged protein.

BP-IgG–Induced BP180 Internalization Is Mediated through a Clathrin-, Caveolae-, and Tyrosine Kinase–Independent Endocytic Pathway

To test whether BP180 internalization is mediated through an endocytic pathway, we performed immunofluorescence analyses using representative molecules for the endocytic pathway. We examined localization of EEA-1 at 1 hour after BP-IgG treatment, and clathrin and caveolin-1 at 2 hours after BP-IgG treatment. Approximately 15% of internalized GFP-BP180 colocalized with EEA-1 (Figure 4A). In

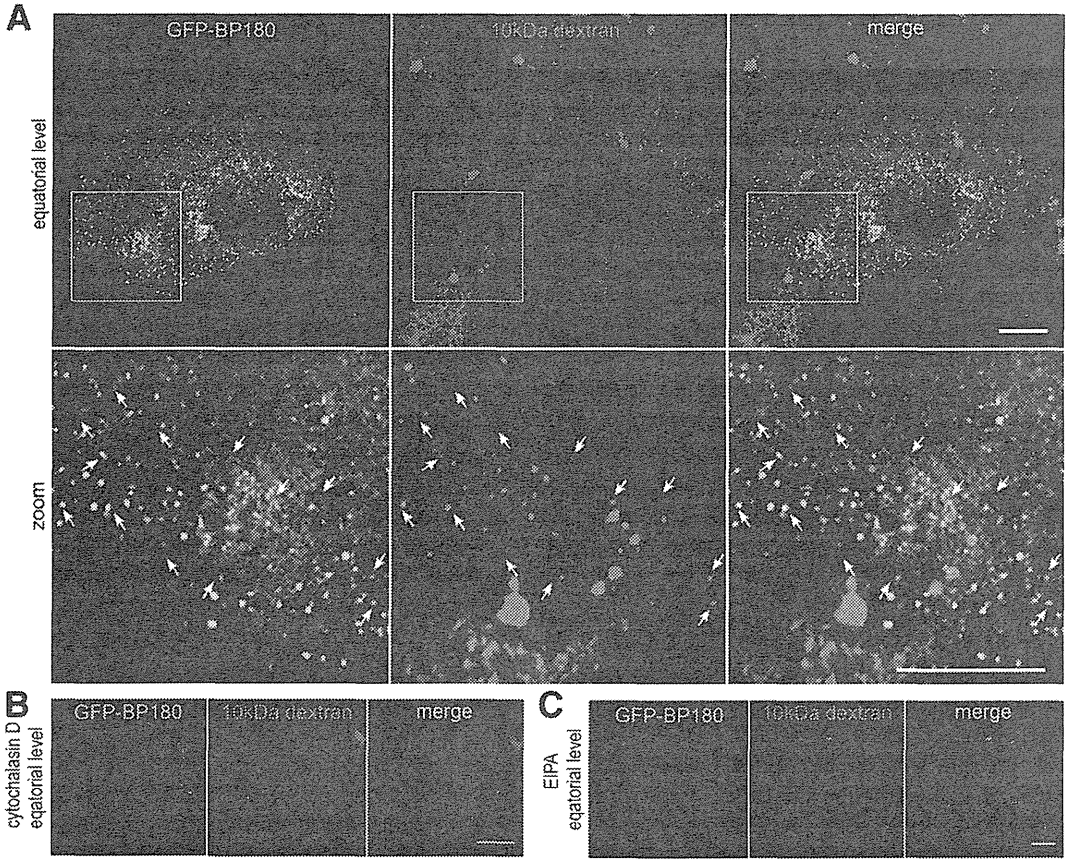

Figure 6 Internalized BP180 colocalizes with the fluid-phase marker. After incubation with BP-IgG and 10-kDa dextran–AF 594 for 10 minutes, GFP-BP180–expressing 804G cells were fixed and viewed. A: Boxed areas are shown at a higher power; 10-kDa dextran–AF 594 was internalized and colocalized with some GFP-BP180 as spot-like structures near the cell surface (**arrows**). Pre-incubation with cytochalasin D (**B**) and EIPA (**C**) inhibited the internalization of GFP-BP180 and dextran. Scale bars: 10 μm.